Nuclear Instruments and Methods in Physics Research A ∎ (∎∎∎∎) ∎∎∎–∎∎∎

Contents lists available at ScienceDirect

Nuclear Instruments and Methods in Physics Research A

journal homepage: www.elsevier.com/locate/nima

Current status and further improvements of the detector for imaging of explosions

V.M. Aulchenko [a], O.V. Evdokov [b], L.I. Shekhtman [a,*], K.A. Ten [c], B.P. Tolochko [b], I.L. Zhogin [b], V.V. Zhulanov [a]

[a] Budker Institute of Nuclear Physics, 11 Lavrentiev Avenue, Novosibirsk 630090, Russia
[b] Institute of Solid-State Chemistry and Mechano-Chemistry, 630090 Novosibirsk, Russia
[c] Lavrentiev Institute of Hydrodynamics, 630090 Novosibirsk, Russian Federation

ARTICLE INFO

Keywords:
GEM
X-ray detector
Detector modelling and simulations

ABSTRACT

The described detector for imaging of explosions (DIMEX) has been designed for the studies of fast processes (explosions, combustion) at synchrotron radiation (SR) beam. DIMEX has been in operation on the SR beam-line on the VEPP-3 electron ring at Budker INP since 2002. DIMEX is based on a one-coordinate gas ionization chamber filled with a Xe–CO_2 (3:1) mixture at 7 atm and active Frisch-grid made of a Gas Electron Multiplier (GEM). The detector has a spatial resolution of 0.2 mm and dynamic range of ~100, which allows one to achieve a signal measurement precision of a few percent. The future possibility to install a similar detector on the SR beam-line on the VEPP-4 electron ring is discussed and the last version of the detector is described.

1. Introduction

The detector for imaging of explosions (DIMEX) has been in operation on the synchrotron radiation (SR) beam-line on the VEPP-3 electron ring at Budker INP since 2002 [1–3]. DIMEX is extensively used for the investigation of material properties under very high temperatures and pressures (i.e., during detonation) [5,6]. Such experiments are performed either by measurement of the absorption of SR beam by an exploding sample (direct absorption experiments), or by measurement of the photon flux scattered at small angles from an exploding sample (SAXS experiments). In both types of experiments, DIMEX allows the measurement of one-coordinate image of the X-ray flux emitted by a single electron bunch and interacting with the sample. The detector produces a "movie" of up to 32 such images corresponding to subsequent bunches. Thus, the effective time resolution of the method is determined by the length of electron bunch in the accelerator and is less than 1 ns.

At present DIMEX is operating on the beam-line with a white SR beam from a 2 T wiggler with an average energy of photons around 20 keV (after passing through Be windows (5 mm) and a sample (1 cm of an explosive)) [1]. This low energy imposes a limit of 1 cm on the sample thickness because otherwise absorption in the sample becomes too strong and limited statistics of transmitted photons do not allow achieving necessary measurement precision. A higher energy of SR beam can be obtained on VEPP-4M with a 5-pole 1.3 T wiggler that is now under development. A dedicated simulation study has been performed to estimate the main parameters of DIMEX for the X-ray spectrum on VEPP-4M. The present paper describes the status of DIMEX performance on VEPP-3 and summarizes the results of simulation studies of possible operation on VEPP-4M.

2. DIMEX status on VEPP-3

DIMEX consists of high pressure gas volume with high voltage drift electrode and Gas Electron Multiplier (GEM) separating the conversion region from the induction gap. The detector design is shown schematically in Fig. 1. The X-ray beam enters the detector volume through a 1 mm wide inlet brass slit and 1 mm thick carbon fibre window or 0.2 mm thick beryllium window (in the last version of the detector). Radiation is absorbed in the conversion region between the drift electrode and the GEM top. The depth of the dead zone between the window and the GEM is 3 mm. The depth of the conversion region between the GEM and the drift electrode is 30 mm. The distance between the drift electrode and the GEM is 1 mm, and the distance between the GEM and the strip board (induction gap) is also 1 mm. Electrons of primary ionization drift towards the GEM, partially penetrate through it and then drift through the induction gap. During the latter phase, there is a charge induced on the strip board. The

*Corresponding author. Tel.: +7 3833 294992; fax: +7 3833 307163.
E-mail address: L.I.Shekhtman@inp.nsk.su (L.I. Shekhtman).

0168-9002/$ - see front matter © 2008 Published by Elsevier B.V.
doi:10.1016/j.nima.2008.12.163

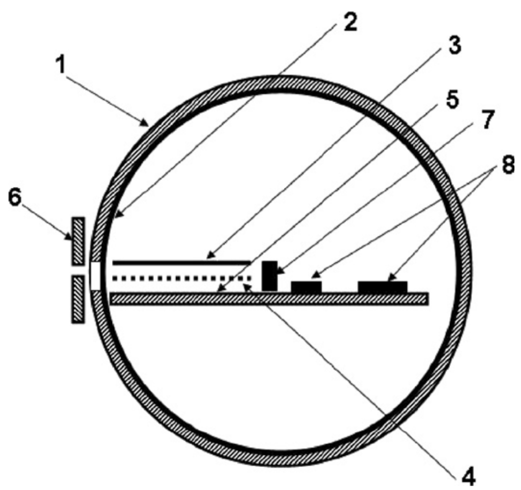

Fig. 1. Schematic view of the DIMEX design: 1—the aluminium box with the inlet window, 2—the 1 mm thick carbon fibre insert, 3—the drift electrode, 4—the GEM, 5—the strip board, 6—the inlet slit, 7—the radiation protection, and 8—the integrator chips and other electronic components.

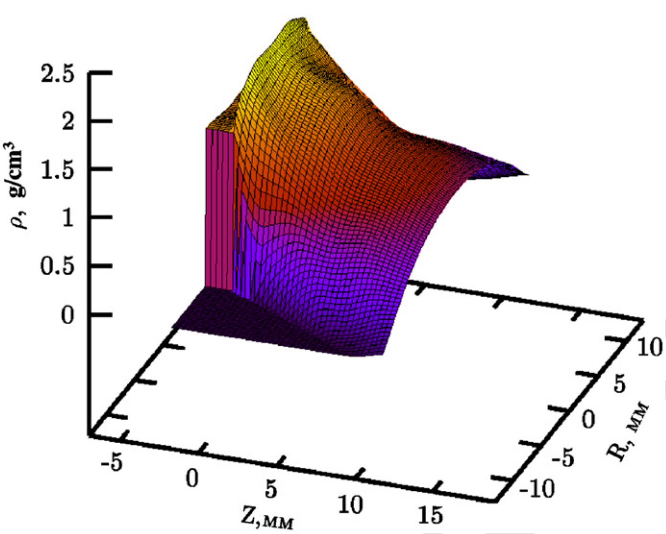

Fig. 2. Reconstructed density map of the exploding sample.

detector is filled with a Xe–CO_2 (3:1) mixture at 7 atm (absolute) and works in a sealed mode.

The active region of the strip structure contains 256 strips in the first detector. In the last version of DIMEX this number has been increased to 512 strips. The strip pitch is 0.1 mm. The length of the strips is equal to 30 mm. Each strip is connected to the input of the integrator chip APC128 [7]. This chip contains 128 channels with an integrator and a 32-cell analogue pipeline in each channel. A charge from the integrator can be stored in any of the pipeline cells. A pipeline can be read out through an analogue multiplexer with the frequency of 10 MHz.

The spatial resolution of DIMEX is determined mostly by the pressure of the operating gas mixture that affects the ranges of photo-electrons, Auger electrons, and fluorescent photons as well as electron diffusion. The resolution (FWHM) is close to 0.2 mm. More detailed discussion about possible reasons of degradation of spatial resolution can be found in Ref. [4].

The signal to noise ratio of the detector reaches 100 [3], which demonstrates the possibility of signal measurement with a precision of a few percent. The maximal signal is limited by the space charge accumulation due to slow positive ions in the drift gap.

The result of one of the direct absorption experiments is shown in Fig. 2, where the density map of the exploding sample is reconstructed [5]. The data are reconstructed from the time evolution of the transmitted signal in one slice, assuming constant speed of the detonation wave. In the figure one can see the undistorted sample at $Z < -5$ mm with a density of $\sim 1.5\,g/cm^3$. At $Z = -5$ mm, the density exceeds $\sim 2.0\,g/cm^3$ due to the detonation and then the sample decays, and the density is steadily decreasing. The most important observation in this kind of experiment is the value of density increase behind the detonation wave, and the exact density profile at the moment of detonation.

Successful operation of DIMEX during the last 5 years proved the power of the method of imaging of radiation from a single electron bunch. However, the detector requires further improvement. For direct absorption experiments, the spatial resolution has to be improved to 50 μm and better, and the dynamic range and precision of signal measurement have to be increased. For both SAXS and direct absorption experiments, a higher frame rate would be useful, though it is limited by the bunch timing of the accelerator. Besides, a transition to higher X-ray energies would be useful for both SAXS and direct absorption experiments. Higher X-ray energies will allow one to study thicker samples with higher densities.

3. Prospects of DIMEX with higher energy SR on VEPP-4M

The energy spectrum of radiation from the 5-pole 1.3 T wiggler that is now under development for the VEPP-4M ring calculated by XOP2.0 has its maximum at ~30 keV. At around 50 keV, its spectral density is about half of the maximum, and the tail spreads up to 100 keV. More detailed discussion about the radiation emitted from VEPP-4M can be found in Ref. [4].

The efficiency of a detector with a 1 mm carbon fibre window of a $1.2\,g/cm^3$ density, a 3 mm deep dead zone of gas, and a 30 mm deep sensitive zone is shown in Fig. 3 as a function of X-ray energy. The efficiency was calculated for a gas mixture of Xe–CO_2 (3:1) at an absolute pressure of 7 atm (the calculation was performed with XOP2.0). Here the efficiency means the probability of absorption of an X-ray photon in the sensitive region of the detector.

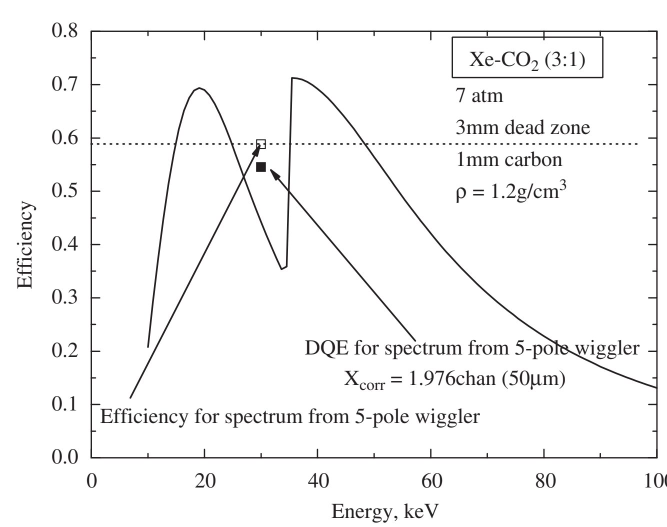

Fig. 3. Efficiency as a function of energy. Efficiency and DQE for radiation with realistic spectrum at VEPP-4M shown at $E = 30$ keV.

Please cite this article as: V.M. Aulchenko, et al., Nucl. Instr. and Meth. A (2009), doi:10.1016/j.nima.2008.12.163

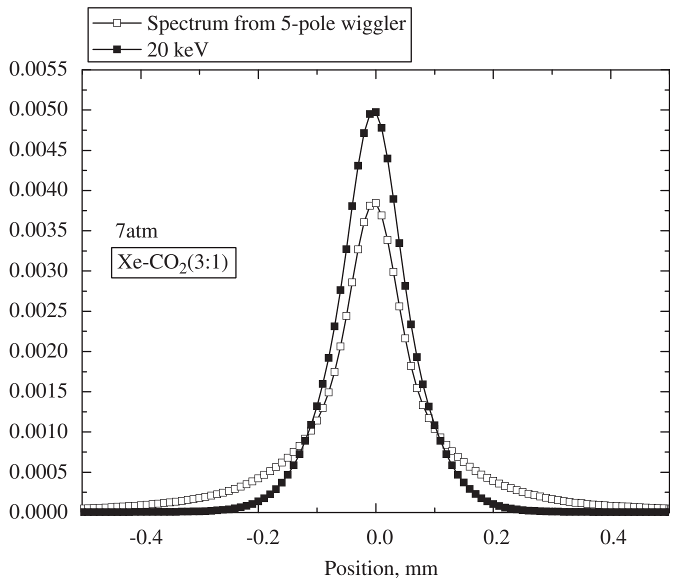

Fig. 4. Comparison of LSF for 20 keV photons and photons with realistic energy spectrum at VEPP-4M with diffusion.

More complicated parameters such as the detector efficiency for realistic energy spectrum, detective quantum efficiency (DQE, see the definition below), and spatial resolution have been obtained by Monte-Carlo simulations. The simulations were performed with the FLUKA2006.3 package [8,9]. FLUKA is a general-purpose tool for the calculation of particle transport and interactions with matter.

For all simulations, the detector model consisted of a carbon fibre window (1 mm thick carbon of a 1.2 g/cm^3 density) and a 1 mm high gas volume with a 3 mm deep dead zone of gas and a 30 mm deep sensitive zone.

The probability of photon absorption in the sensitive region does not characterize the detector performance completely. This value does not take into account the sources of noise different from Poisson fluctuations of the detected quanta. A complete measure of detector performance is DQE [10]. DQE is defined as

$$\mathrm{DQE} = \frac{\mathrm{SNR}_{out}^2}{\mathrm{SNR}_{in}^2} \quad (1)$$

where SNR_{out} is the signal to noise ratio at the output of the detector and SNR_{in} is the signal to noise ratio at the input of the detector. More detailed description of the method used to calculate DQE can be found in Ref. [4].

The spatial resolution of DIMEX is characterized by the line spread function (LSF) that was obtained by the simulation. Electron diffusion was added to the simulation results by convolution. The comparison between the LSF with and without electron diffusion demonstrates that the spatial resolution of DIMEX is mostly determined by diffusion [4].

Complete LSF is compared in Fig. 4 for a 20 keV photon beam and for X-rays with realistic energy spectrum from the wiggler at VEPP-4M. The difference between these two LSFs is only in a wider halo for the case of the spectrum at VEPP-4M. FWHM in both cases is about 170 μm, which agrees very well with the experimental result (see Ref. [3]).

An alternative to the gaseous detector can be a solid-state device. Simulations have been performed with a Si detector 1 cm long in the beam direction and 0.3 mm thick in the perpendicular direction. The efficiency for photons with the spectrum from 5-pole 1.3 T wiggler at VEPP-4M in the 1 cm thick Si detector is equal to ~81% while DQE is ~42% due to the fluctuations of deposited energy because of high probability of Compton scattering. The spatial resolution of Si detector is much better than that of the gaseous DIMEX. The simulation results demonstrated FWHM of the LSF of ~20 μm. More detailed discussion of these results can be found in Ref. [4].

4. Conclusions

Several years of experience with DIMEX on the SR beam-line on VEPP-3 have proven the method of imaging of radiation from separate electron bunches to be a very powerful tool. However, in spite of successful application of the detector, further improvement of the method is desirable. The development of the new 5-pole 1.3 T wiggler on VEPP-4M and the construction of the new dedicated SR beam-line will allow increasing the energy and thus the thickness of samples under study. The simulation study performed in the present work demonstrates that the present detector will keep its parameters with a higher energy SR beam on VEPP-4M. The spatial resolution will stay at 0.2 mm (FWHM) and DQE will be around 50%.

Gaseous technology limits the spatial resolution of DIMEX and the maximal X-ray flux that this detector can withstand. Further improvement of both parameters can be achieved with a silicon microstrip detector positioned at a small angle to the beam. The simulation shows that if a beam crosses the Si detector within a 1 cm length, the DQE for the X-ray spectrum from the VEPP-4M wiggler is close to that of the gaseous DIMEX. The spatial resolution, however, can be much better if a proper segmentation is done, because the LSF of the Si detector before the application of any strip readout structure is about 20 μm wide (FWHM).

References

[1] V. Aulchenko, P. Papushev, S. Ponomarev, L. Shekhtman, V. Zhulanov, J. Synchrotron Rad. 10 (2003) 361.
[2] V. Aulchenko, O. Evdokov, S. Ponomarev, L. Shekhtman, K. Ten, B. Tolochko, I. Zhogin, V. Zhulanov, Nucl. Instr. and Meth. 513 (1–2) (2003) 388.
[3] V. Aulchenko, V. Zhulanov, L. Shekhtman, B. Tolochko, I. Zhogin, O. Evdokov, K. Ten, Nucl. Instr. and. Meth. A 543 (1) (2005) 350.
[4] V.M. Aulchenko, O.V. Evdokov, L.I. Shekhtman, K.A. Ten, B.P. Tolochko, I.L. Zhogin, V.V. Zhulanov, J. Instr. 3 (2008) P05005.
[5] E.R. Pruuel, L.A. Merzhievskii, K.A. Ten, P.I. Zubkov, L.A. Luk'yanchikov, B.P. Tolochko, A.N. Kozyrev, V.V. Litvenko, Combust. Explos. Shock Wave 43 (3) (2007) 355.
[6] V.M. Titov, B.P. Tolochko, K.A. Ten, L.A. Lukyanchikov, E.R. Pruuel, Diam. Relat. Mater. 16 (12) (2007) 2009.
[7] R. Horisberger, D. Pitzl, Nucl. Instr. and Meth. A 326 (1993) 92.
[8] A. Fasso, A. Ferrari, J. Ranft, P.R. Sala, FLUKA: a multi-particle transport code, CERN-2005-10, INFN/TC-05/11, SLAC-R-773, 2005.
[9] A. Fasso, A. Ferrari, S. Roesler, P.R. Sala, G. Battistoni, F. Cerutti, E. Gadioli, M.V. Garzelli, F. Ballarini, A. Ottolenghi, A. Empl, J. Ranft, The physics models of FLUKA: status and recent developments, in: Computing in High Energy and Nuclear Physics 2003 Conference (CHEP2003), La Jolla, CA, USA, March 24–28 2003 (paper MOMT005), eConf C0303241, 2003, arXiv:hep-ph/0306267.
[10] J.C. Dainty, R. Shaw, Image Science: Principles, Analysis, and Evaluation of Photographic-Type Imaging Processes, Academic Press, New York, 1974.

Please cite this article as: V.M. Aulchenko, et al., Nucl. Instr. and Meth. A (2009), doi:10.1016/j.nima.2008.12.163